American Mineralogist, Volume 81, pages 375–384, 1996

Magnetic properties of the magnetite-spinel solid solution: Curie temperatures, magnetic susceptibilities, and cation ordering

RICHARD J. HARRISON AND ANDREW PUTNIS*

Department of Earth Sciences, University of Cambridge, Downing Street, Cambridge CB2 3EQ, U.K.

ABSTRACT

Curie temperatures (T_C) of the $(Fe_3O_4)_x(MgAl_2O_4)_{1-x}$ solid solution have been determined from measurements of magnetic susceptibility (χ) vs. temperature. The trend in T_C vs. composition extrapolates to 0 K at $x = 0.27$. This behavior is rationalized in terms of the trend in cation distribution vs. composition suggested by Nell and Wood (1989), with Fe occurring predominantly on tetrahedral sites for $x < 0.27$.

High-temperature χ-T curves are nonreversible because of the processes of cation ordering and exsolution, which occur in the temperature range 400–650 °C. The Curie temperature of single-phase material is shown to be sensitive to the state of nonconvergent cation order, with a difference in T_C of more than 70 °C being observed between a sample quenched from 1400 °C and the same sample after heating to 650 °C. This interaction between magnetic and chemical ordering leads to thermal hysteresis behavior such that T_C measured during heating experiments is approximately 10 °C higher than that measured during cooling. The hysteresis is due to a reversible difference in the state of cation order during heating and cooling caused by a kinetic lag in the cation-ordering behavior.

Samples with compositions in the range $0.55 < x < 0.7$ undergo exsolution to a mixture of ferrimagnetic and paramagnetic phases after heating to 650 °C. Room-temperature hysteresis loops of the starting material and the high-temperature experiment products are compared. All starting materials are multidomain with coercivities $H_C < 1.26$ mT and $M_{rs}/M_s < 0.051$. Samples that exsolved during the experiments have coercivities up to 20 mT and M_{rs}/M_s up to 0.36. This change in hysteresis properties is caused by grain subdivision during exsolution and implies a transition in the magnetic domain state from multi- to single-domain.

INTRODUCTION

The magnetic properties of solid solutions are sensitive to the processes of oxidation, cation ordering, and subsolidus exsolution. Both in nature and in laboratory experiments these processes can occur concurrently, resulting in complex microstructures and a magnetic signature that is characteristic of the mineral processes that occurred. In rock magnetism it is the magnetic properties of minerals responsible for natural remanent magnetizations that are of interest. Studying the interaction between cation ordering, exsolution, and magnetism helps us to understand the acquisition, alteration, and stability of natural magnetizations over geological time. In mineral physics magnetic properties of complex solid solutions provide a sensitive probe for the study of intrinsic mineral properties and kinetic processes.

This paper is the second in a series detailing the magnetic properties of the magnetite-spinel solid solution $(Fe_3O_4)_x(MgAl_2O_4)_{1-x}$ (Harrison and Putnis 1995). The general aims of the project are to investigate the interaction between magnetism and the processes of subsolidus exsolution and nonconvergent cation ordering. Exsolution microstructures are often responsible for high coercivities in naturally occurring magnetic minerals such as the titanomagnetite solid solution (Tucker and O'Reilly 1980; Shive and Butler 1969; Price 1980; Evans and Wayman 1974). Although titanomagnetite is the most important cause of remanence in rocks, it is not possible to study the development of subsolidus exsolution microstructures in synthetic titanomagnetite because of the low temperatures required to produce spinodal decomposition. However, the general principles of the relationship between magnetism, chemical composition, microstructure, and cation ordering can be studied in related systems. The magnetite-spinel solid solution is a more suitable system in that the chemical solvus has a consolute point near 1000 °C (Mattioli and Wood 1988) and there are extensive changes in the degree of nonconvergent cation order as a function of temperature (Nell and Wood 1989; Nell et al. 1989).

In a previous paper (Harrison and Putnis 1995) we detailed low-temperature hysteresis properties of the homogeneous solid solution. The trend in saturation magnetization vs. composition can be understood in terms of the distribution of Fe atoms between tetrahedral (A) and

* Permanent address: Universität Muenster, Institut für Mineralogie, Correnstrasse 24, 48149 Münster, Germany.

0003–004X/96/0304–0375$05.00

octahedral (B) sites, the net magnetization being the difference between the A and B sublattice magnetizations (Brown et al. 1993). The results showed that for $x > 0.3$ the solid solution is ferrimagnetic with the B sublattice magnetization greater than the A sublattice magnetization. For $x < 0.3$ the solid solution is ferrimagnetic with the A sublattice magnetization greater than the B sublattice magnetization. The $x = 0.3$ composition is a compensation point corresponding to an antiferromagnetic spin structure with A and B sublattice magnetizations equal. The compensation point is associated with a pronounced peak in the coercivity of 700 mT, which is related to the presence of fine-scale heterogeneities in composition and degree of cation order.

There is a discrepancy between the position of the compensation point reported by Harrison and Putnis (1995) for samples quenched from 1400 °C and the position predicted by the Nell and Wood (1989) model for an equilibration temperature of 1400 °C. This discrepancy is due to cation reordering, which occurs when quenching from high temperatures. The position of the compensation point in quenched samples is a function of the kinetics of cation reordering and cannot be predicted directly from equilibrium models. The observed compensation point at $x = 0.3$ is consistent with Nell and Wood (1989) if a kinetic closure temperature of 1200 °C is assumed.

Other experimental work on this solid solution includes measurements of lattice parameters, activities, Curie temperatures, room-temperature low-field magnetization, and cation distribution vs. composition (Mattioli et al. 1987; Mattioli and Wood 1988; Nishitani 1981; Nell et al. 1989). This paper presents the results of alternating-field susceptibility measurements on synthetic samples of the magnetite-spinel solid solution, initially quenched from 1400 °C. We demonstrate that susceptibility measurements can be used to monitor changes in the Curie temperature associated with both compositional changes and changes in the degree of cation order.

Theoretical background

Crystal structure and cation distributions of magnetic spinels

Magnetite ($Fe^{2+}Fe_2^{3+}O_4$) and spinel ($MgAl_2O_4$) are both cubic spinels with space-group $Fd\bar{3}m$ and eight formula units per unit cell. The 32 O atoms per unit cell are in an approximately close-packed arrangement with cations occupying eight tetrahedral (A) sites and 16 edge-sharing octahedral (B) sites. At room temperature $MgAl_2O_4$ has the normal spinel cation distribution with 8 Mg atoms occupying A sites and 16 Al atoms on B sites. Fe_3O_4 has the inverse spinel cation distribution at room temperature with 8 Fe^{3+} ions occupying A sites and 8 Fe^{3+} + 8 Fe^{2+} ions occupying B sites. At elevated temperatures cations become progressively disordered over both A and B sites (Peterson et al. 1991; Wood et al. 1986; Carpenter and Salje 1994; Trestman-Matts et al. 1983). The process of nonconvergent cation ordering is a common phenomenon in spinels and has been discussed in detail in the literature (Carpenter et al. 1994; O'Neill and Navrotsky 1984; Nell and Wood 1989; Sack and Ghiorso 1991; Stephenson 1969). The term nonconvergent means that there is no symmetry change involved in ordering cations between A and B sites.

The distribution of cations between octahedral and tetrahedral sites for the $(Fe_3O_4)_x(MgAl_2O_4)_{1-x}$ solid solution has been experimentally determined at 1000 °C (Nell et al. 1989), and a thermodynamic model describing the temperature dependence of cation distribution has been proposed (Nell and Wood 1989). The solid solution has a solvus at temperatures below 1000 °C (Mattioli and Wood 1988). Exsolution occurs within the quaternary system Fe_3O_4-$FeAl_2O_4$-$MgFe_2O_4$-$MgAl_2O_4$, but tie-lines joining Fe-rich and Fe-poor phases remain close to the binary join Fe_3O_4-$MgAl_2O_4$ (Lehmann and Roux 1986).

The spin-only magnetic moments associated with Fe^{2+} and Fe^{3+} ions are 4 and 5 μ_B, respectively ($1\ \mu_B = 9.27 \times 10^{-24}$ Am^2). Below the Curie temperature (T_C) of a magnetic spinel Fe atoms on B sites have their moments aligned parallel to each other but antiparallel to those on A sites. The net saturation magnetization is given by the difference between the octahedral and tetrahedral sublattice magnetizations (Stephenson 1972). If the sublattice magnetizations are unequal then the net magnetization is nonzero and the material is ferrimagnetic. For example, magnetite with the inverse cation distribution has a net moment of 4 μ_B. If the sublattice magnetizations are equal, then the net magnetization is zero and the material is antiferromagnetic.

Temperature dependence of magnetic susceptibility (χ)

Here we present a brief outline of the theory relevant to the interpretation of susceptibility-temperature curves. For a detailed description of rock and mineral magnetism the reader is referred to O'Reilly (1984). Magnetic susceptibility (χ) describes the response of a material to an applied magnetic field. The magnetization per unit mass M (Am^2/kg) acquired by a material in a field H (A/m) defines susceptibility using the equation $\chi = M/H$ (m^3/kg). If H is an alternating field, then the response of the material may not be in phase with the field. In this case χ has an imaginary component and hence $\chi = \chi' + i\chi''$. In the majority of cases only the real component of susceptibility is considered and this is denoted χ in what follows.

Below T_C the temperature dependence of χ may be understood in terms of the relationship $\chi(T) \propto M_s(T)/K(T)$, where M_s is the spontaneous magnetization and K is the magnetic anisotropy. Both M_s and K decrease with increasing temperature. At low temperatures these two effects cancel and χ remains roughly constant. As $T \rightarrow T_C$ both M_s and $K \rightarrow 0$. If K decreases at a faster rate than M_s, then thermal fluctuations at T close to T_C lead to enhanced susceptibility (Dunlop 1974). This is known as the Hopkinson effect. Above T_C, M_s is zero and the material displays only paramagnetic susceptibility, which falls to zero rapidly as $\chi \propto 1/(T - T_C)$. This sharp decrease

TABLE 1. Curie temperatures of synthetic spinels

Sample	x^*	T_C expt. 1 (°C)		T_C expt. 2 (°C)	
		Heating	Cooling	Heating	Cooling
SP15	1	584.4	583.9	—	—
SP18	0.9	517	517.3	—	—
SP14	0.81	470.7	488	513.8	489.3
SP17	0.71	355.3	515.4**	526.8**	516.5**
SP13	0.609	283.2	518.9**	528.3**	518**
SP20	0.55	170.6	517.8**	—	—
SP12	0.51	107.6	175.7, 502.6†	179.11, 513.7†	181.9, 507.8†
SP9	0.43	—	467.1**	479.8**	468.2**
SP10	0.36	−110.8	—	—	—
SP6	0.3	−212.7	—	—	—
SP9	0.43	−9.9	—	—	—

* Mole-fraction magnetite defined by ideal formula unit $(Fe_3O_4)_x(MgAl_2O_4)_{1-x}$.
** Susceptibility remains finite up to ~525 °C.
† Sample remains two phase, both Curie temperatures given.

in χ provides an accurate determination of T_C and hence an insight into changes in composition and degree of cation order that occur during the measurements.

Experimental and analytical procedures

Synthesis

The starting materials for all syntheses were 99.9% pure Fe_2O_3 and MgO, and Al_2O_3 prepared by firing $AlCl_3 \cdot 6H_2O$ for 2 h at 400 °C, 5 h at 700 °C, and 1 h at 900 °C. The oxides were weighed in stoichiometric proportions, ground together, and pressed into pellets. The pellets were then fired at 1400 °C for periods between 3 and 5 d in a vertical-tube gas-mixing furnace under controlled f_{O_2} (Nafziger et al. 1971). A value of $\log(f_{O_2}) = -4.2$ was chosen to yield stoichiometry in the magnetite component of the solid solution (Dieckmann 1982). Samples were quenched from 1400 °C by dropping directly from the furnace into water. Starting materials were characterized by X-ray diffraction, electron microprobe analysis, and SEM and TEM techniques. A detailed description of the synthesis technique and sample characterization is given by Harrison and Putnis (1995). All samples quenched from 1400 °C are single phase.

Magnetic measurements

Measurements of high-temperature alternating-field susceptibility were made in air using a KAPPA susceptibility bridge. Individual pellets of synthetic material with masses ranging from 9 to 46 mg were placed in an open test tube inside a water-cooled furnace. Measurements of susceptibility were made every 15–20 s while the temperature was ramped from room temperature to 650 °C and back to room temperature at a rate of 11 °C/min. Temperatures were measured with a Pt-Rh thermocouple placed directly next to the sample. The total time for each experiment is approximately 1.9 h. High-temperature experiments were performed on samples with $x \geq 0.43$, i.e., those with Curie temperatures near or above room temperature.

Measurements of low-temperature alternating-field susceptibility were made with a Lakeshore susceptometer. Several pellets of material (total sample mass between 81 and 126 mg) were packed in a gelatin capsule and placed in a sample chamber with a helium atmosphere. Temperature was controlled with a refrigerator unit. Measurements of both real and imaginary components of magnetic susceptibility were made in the temperature range 20–300 K (−253 to 27 °C). Only samples with Curie temperatures below room temperature were measured using the Lakeshore susceptometer.

Low-field DC magnetic behavior of samples SP9 and SP5 (see Table 1) was measured with a Quantum Design MPMS1 SQUID magnetometer. The samples were cooled to 20 K in zero field. For SP9, magnetization in a constant field of 5 mT was measured as a function of temperature in 10 K steps to 300 K. The temperature was equilibrated at each step prior to measurement. This measurement provided the only determination of T_C for sample SP9. For SP5 magnetization was measured in temperature-sweep mode with a heating rate of 5 °C/min.

Susceptibility and low-field magnetization rapidly fall to zero above T_C. Values of T_C were determined from the data sets by linearly extrapolating the χ-T curves to the $\chi = 0$ axis. Extrapolation was performed by fitting a straight line by least squares to the data points immediately surrounding the point of inflection. This procedure was performed for both heating and cooling parts of the χ-T curves.

Room-temperature hysteresis loops of starting materials with $x \geq 0.5$ and the products of high-temperature experiments displaying nonreversible χ-T curves were measured using a vibrating sample magnetometer. All samples saturated in the maximum applied field of 800 mT. Values of the room-temperature saturation magnetization (M_s) were determined by linearly extrapolating the high-field portion of the loop to the $H = 0$ axis. The value of the saturation remanent magnetization (M_{rs}) and coercivity (H_c) were taken directly from the hysteresis loops.

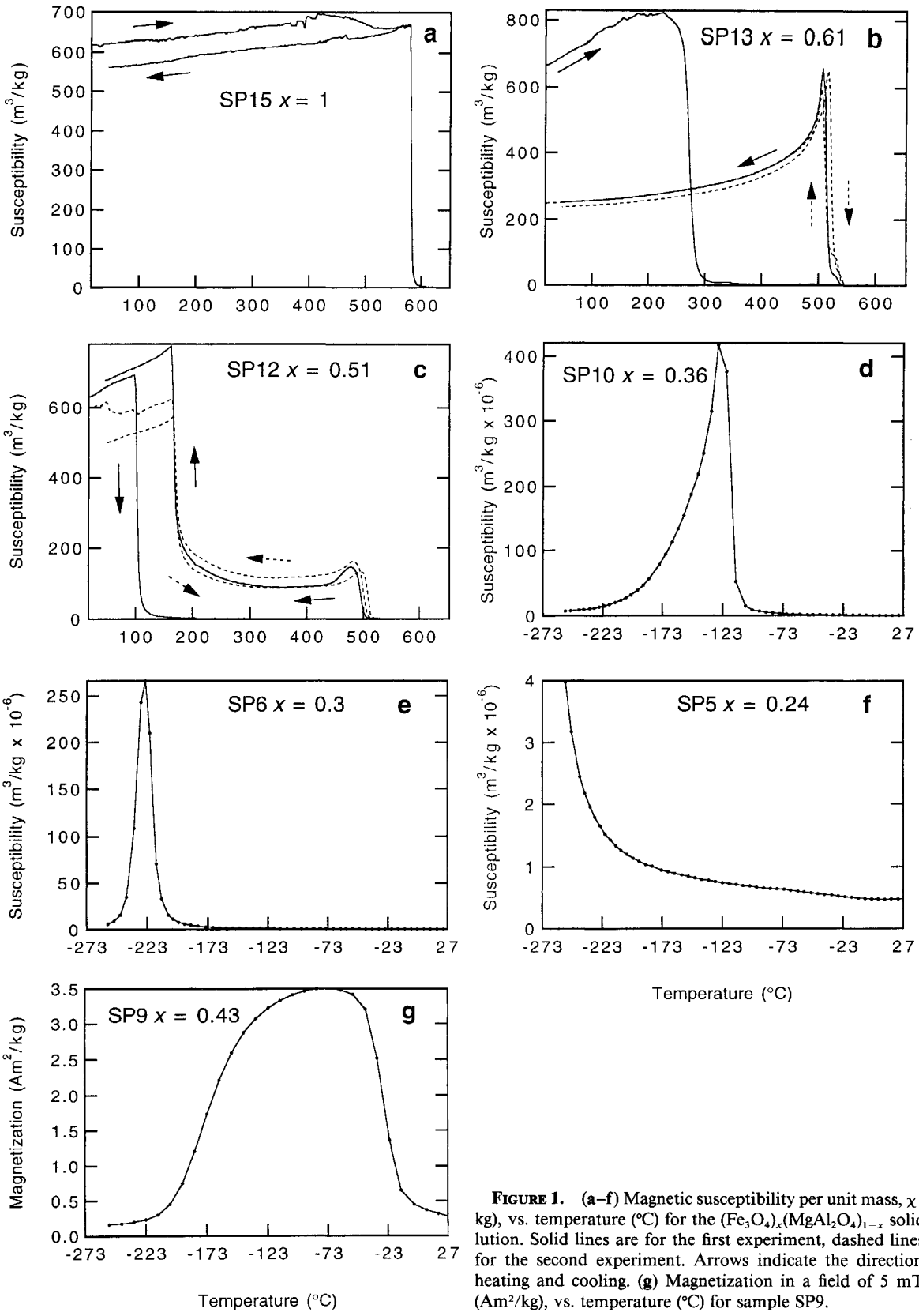

FIGURE 1. (**a–f**) Magnetic susceptibility per unit mass, χ (m^3/kg), vs. temperature (°C) for the $(Fe_3O_4)_x(MgAl_2O_4)_{1-x}$ solid solution. Solid lines are for the first experiment, dashed lines are for the second experiment. Arrows indicate the directions of heating and cooling. (**g**) Magnetization in a field of 5 mT, M (Am^2/kg), vs. temperature (°C) for sample SP9.

Results and discussion

Initial Curie temperatures of the homogeneous solid solution

T_C data for all heating and cooling experiments are presented in Table 1. Selected χ-T curves and the low-temperature DC magnetization experiment for SP9 are presented in Figure 1. Figure 1a shows the behavior in the pure Fe_3O_4 end-member. A sharp decrease in χ occurs at the Curie temperature T_C = 584.4 °C (see Table 1). This value corresponds to the magnetic transition in stoichiometric magnetite (Readman and O'Reilly 1972), and hence we suggest that although oxidation at the rim of the sample pellet cannot be ruled out, the bulk of the sample remains unoxidized during the timescale of the experiments. This view is supported by the reversible nature of the magnetic transition after heating to 650 °C.

Figures 1b–1g show the behavior for selected intermediate members of the solid solution. If two experiments were performed on the same sample, the first experiment is shown as a solid curve and the second experiment as a dashed curve. The behavior of these samples is complicated because of the processes of cation ordering and exsolution that occur on heating. The rate of these two processes is slow below 400 °C, and hence the decrease in χ during the first heating experiment is associated with the magnetic transition in homogeneous material quenched from 1400 °C. Nonreversible changes in cation order and composition occur on heating above 400 °C resulting in complex χ-T behavior. These curves are discussed in detail in later sections.

Curie temperatures vs. composition for the first heating experiments are listed in Table 1 and are shown in Figure 2 along with the T_C data of Nishitani (1981). Samples with $x < 0.3$ display only paramagnetic susceptibility at temperatures above 20 K (Fig. 1f). These samples exhibit hysteresis at 4.4 K (Harrison and Putnis 1995), and therefore we conclude that T_C for $x < 0.3$ lies in the temperature range 4.4–20 K as indicated by the limits in Figure 2. There is a clear trend in the variation of T_C with composition for $x > 0.3$. The solid line is a least-squares fit to the T_C-x data ($x > 0.3$) with a third-order polynomial function T_C (°C) = $-853 + 2410x - 970x^2$. This function extrapolates to 0 K at $x = 0.27$. Nishitani (1981) measured T_C on samples of the solid solution annealed and quenched from 1200 °C. Differences in the trend of T_C vs. composition between the present work and that of Nishitani (1981) may reflect either differences in nonstoichiometry in the samples or differences in cation order due to quenching from 1200 °C as opposed to 1400 °C.

To interpret the variation of Curie temperature with composition (Fig. 2) we must first understand the nature of the interactions that are responsible for magnetic ordering. A detailed discussion of the atomic basis for magnetic ordering in oxide spinels is given by O'Reilly (1984). Fe^{2+} and Fe^{3+} ions have net magnetic moments because of the presence of unpaired d-orbital electrons. When the

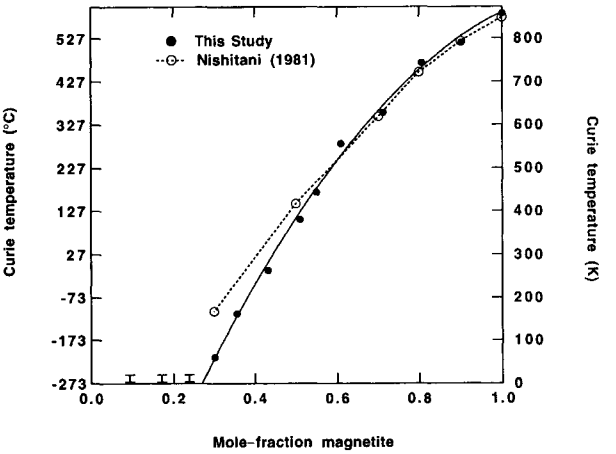

FIGURE 2. Curie temperature, T_C (°C), vs. composition. Solid circles are the data of this study taken from χ-T curves for the first heating experiment. Limits for $x < 0.3$ represent the possible range in T_C for these compositions (4.4–20 K). The solid line is a fit to the data with $x \geq 0.3$ T_C (°C) = $-853 + 2410x - 970x^2$. Open circles and dashed line are the data of Nishitani (1981).

electron orbitals from neighboring atoms overlap, the magnetic moments interact to cause the energy of the moments to depend upon their relative orientation. This exchange interaction is described by the equation $E_{ex} = -2JS^2\cos\theta$, where E_{ex} is the exchange energy, J is the exchange constant for two identical atoms, S is proportional to the magnetic moment of the atoms, and θ is the angle between the moments. If $J > 0$, then the moments align parallel to one another (ferromagnetic ordering), and if $J < 0$, then the moments align antiparallel (antiferromagnetic ordering). In magnetic spinels there is little direct overlap of Fe ion orbitals, but superexchange interactions do occur by means of O atoms. Fe atoms occur on both A and B sites, and hence we consider three superexchange constants: J_{AA}, J_{BB}, and J_{AB}. Magnetic ordering in Fe-rich spinels is dominated by the negative J_{AB} interaction, which leads to the ferrimagnetic behavior discussed earlier.

The strength of the superexchange interaction determines the Curie temperature. The decrease in T_C with increasing mole-fraction $MgAl_2O_4$ is due to dilution of the J_{AB} interaction by nonmagnetic Mg and Al atoms. Similar behavior is seen in the titanomagnetite solid solution because of the dilution of Fe_3O_4 by nonmagnetic Ti atoms (Stephenson 1972). At $x = 0.3$ there is an abrupt change in the T_C-x trend, which implies an abrupt change in the strength of the superexchange interaction. This composition has been previously identified with a compensation point in the trend of saturation magnetization vs. composition (Harrison and Putnis 1995). Assuming a kinetic closure temperature of 1200 °C for samples quenched from 1400 °C, the cation distribution suggested

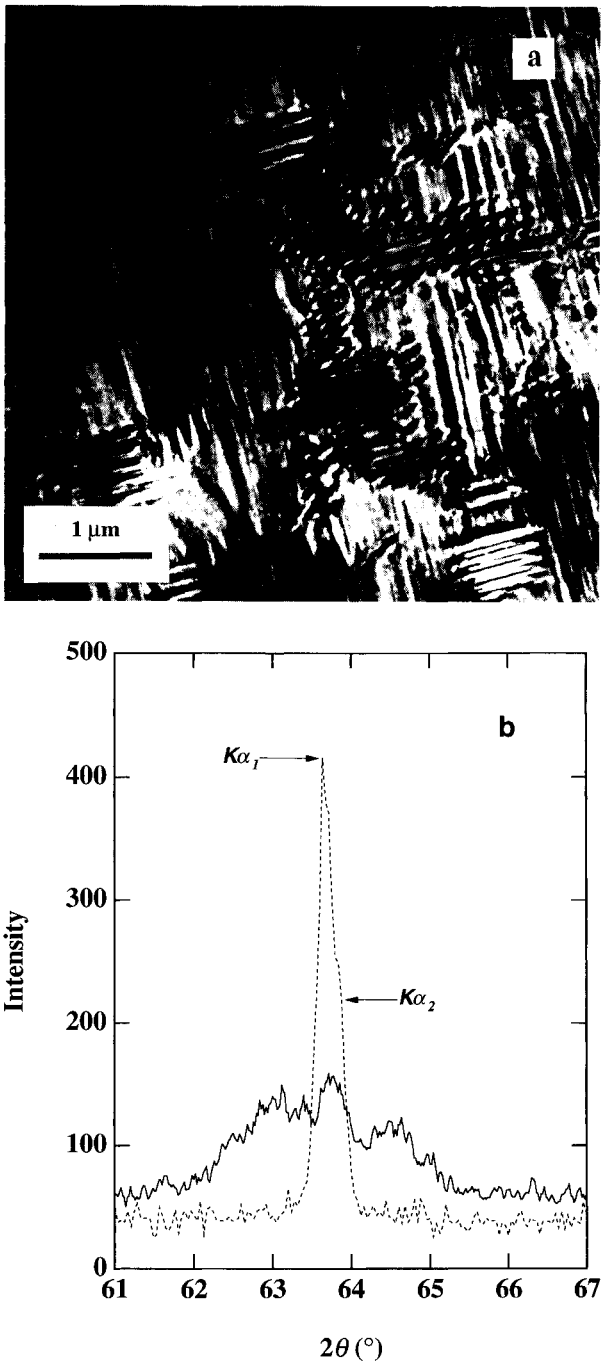

FIGURE 3. (a) Transmission electron micrograph of sample SP20 after a single high-temperature susceptibility experiment. (b) Smoothed XRD trace of the 440 reflection for sample SP20 after a single high-temperature susceptibility experiment (solid line) and the same reflection in the starting material (dashed line).

by Nell and Wood (1989) has Fe located predominantly on B sites for $x > 0.3$, leading to ferrimagnetic ordering. The compensation point at $x \approx 0.3$ has both magnetic sublattices equal and hence no net magnetization. For $x < 0.3$, Fe is distributed predominantly on A sites, causing a small increase in the net magnetization. The strength of the J_{AA} interaction is very much less than that of the J_{AB} interaction. The abrupt change in T_C vs. x at $x \approx 0.3$ is entirely consistent with the change in Fe distribution suggested by Nell and Wood (1989) and is caused by Fe atoms being located predominantly on tetrahedral sites, hence reducing the strength of the superexchange interaction.

Nonreversibility of high-temperature χ-T curves: Exsolution

The nonreversible behavior of the high-temperature χ-T curves can be understood in terms of the changes in composition and degree of cation order that occur at temperatures greater than approximately 400 °C. In Figure 1b (SP13 $x = 0.61$) the first decrease in χ at 283 °C is associated with T_C for the homogeneous solid solution. The cooling curve, however, shows a single magnetic transition with $T_C = 519$ °C. Samples SP17 ($x = 0.71$) and SP20 ($x = 0.55$) show similar behavior (Table 1). The increase in T_C observed in these samples after heating to 650 °C is caused by subsolvus exsolution, which results in an intergrowth of Fe-rich and Fe-poor phases. Sample SP20 was investigated by both XRD and TEM techniques. The microstructure in this sample after a single high-temperature susceptibility experiment is shown in Figure 3a and consists of intersecting lamellae parallel to {100}. A comparison of the 440 XRD peak profile for sample SP20 before and after the high-temperature experiment is shown in Figure 3b. The exsolved sample consists of three spinel phases corresponding to an Fe-rich phase, an Fe-poor phase, and the original bulk phase. If we assume that exsolution occurs close to the $(Fe_3O_4)_x(MgAl_2O_4)_{1-x}$ binary join, then the Fe-rich phase with $T_C = 519$ °C corresponds to a composition $x \approx 0.89$ (Fig. 2). T_C for the Fe-poor phase is below room temperature.

Further demonstration of exsolution in these samples is provided by a comparison of room-temperature hysteresis properties before and after the high-temperature experiments. Hysteresis loops for sample SP13 are presented in Figure 4, and hysteresis parameters are listed in Table 2. All starting materials show multidomain behavior with $H_c \leq 1.26$ mT and $M_{rs}/M_s \leq 0.051$. After heating, samples SP13, SP17, and SP20 display hysteresis properties similar to those of randomly oriented single-domain grains (Stoner and Wohlfarth 1948). H_c is in the range 13.3–19.9 mT, and M_{rs}/M_s is in the range 0.28–0.36. The ideal value of the ratio M_{rs}/M_s for noninteracting single-domain grains is 0.5. The lower value observed here is probably caused by magnetostatic interaction between grains (Davis and Evans 1976). The pronounced Hopkinson susceptibility peak observed at T_C for the exsolved phase is further evidence of single-domain behavior (Dunlop 1974). The transition from multi- to single-domain behavior in response to subsolvus exsolution was recognized earlier in natural titanomagnetite (Evans and Wayman 1974; Price 1980) and

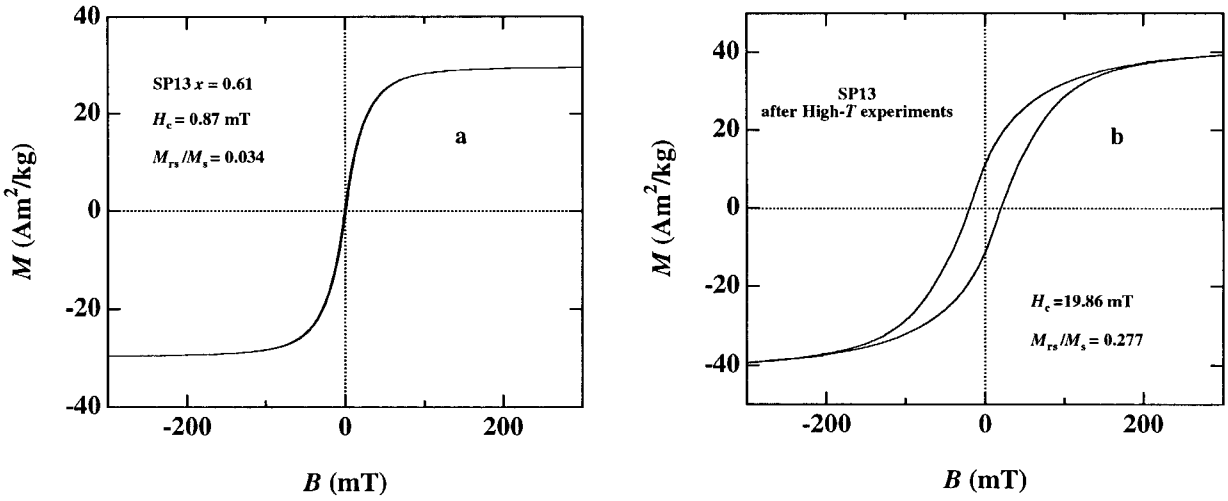

FIGURE 4. Room-temperature magnetization per unit mass, M (Am²/kg), vs. applied field, B (mT), for (a) sample SP13 starting material as quenched from 1400 °C, (b) sample SP13 after heating to 650 °C in KAPPA susceptibility bridge.

is caused by subdivision of large multidomain grains by {100} lamellae of a paramagnetic phase. This results in a cubic array of interacting magnetic grains with diameters below the threshold size for single-domain behavior. Estimates of the value of the multidomain to single-domain threshold size vary but are on the order of 0.05 μm (Dunlop 1973). However, this value may vary significantly if there is strong interaction between magnetic particles. The role of exsolution in producing technological materials with high coercivities has been well studied (Zijlstra 1982; Livingston 1981).

Nonreversibility of high-temperature χ-T curves: Cation ordering

The behavior of sample SP12 (x = 0.51) is shown in Figure 1c. T_C for the homogeneous phase is initially 107.6 °C. After heating to 650 °C partial exsolution of an Fe-rich phase occurs with T_C = 502.6 °C. Exsolution proceeds to a much lesser extent in this sample than for samples with $x \geq 0.55$, and there is a strong magnetic signal from the remaining bulk phase. T_C for the remaining bulk phase measured during cooling is 175.7 °C. There is a difference of approximately 70 °C between T_C for the bulk phase measured during the first heating experiment and that measured after the sample was heated to 650 °C. Given that partial exsolution of an Fe-rich phase has occurred the composition of the remaining bulk phase is poorer in Fe than before. This should lead to a decrease in Curie temperature rather than the observed increase. There are no significant increases in H_c or M_{rs}/M_s after the heating experiments (Table 2), implying that the bulk of the sample remains homogeneous. Hence, the increase in T_C is not produced by the change in the composition of the bulk phase. It is unlikely that the observed increase in T_C is caused by oxidation of the sample because, as discussed earlier, the χ-T curve for pure Fe_3O_4 is reversible (Fig. 1a) and shows no evidence that bulk oxidation occurred during the experiments.

We conclude that the increase in T_C is due to a large difference in the state of nonconvergent cation order between the sample that is initially quenched from 1400 °C and the same sample subsequently heated to 650 °C. This interpretation requires careful consideration of the cation ordering and kinetic behavior of quenched samples. Our framework for the description of nonconvergent cation ordering in spinels follows that of Carpenter et al. (1994). We describe the state of cation order in terms of an order parameter Q that takes a value of Q = 0 for complete cation disorder between A and B sites and a value of Q = 1 for complete order at T = 0 K. A sample annealed at 1400 °C is relatively disordered and has a low value of Q. Significant cation reordering can occur during quenching from high temperatures (Wood et al. 1986; Milliard et al. 1992). It is found that spinels annealed at temperatures >900–1000 °C reorder during the quench to yield a constant value of Q equivalent to the equilibrium value

TABLE 2. Hysteresis properties of synthetic spinels before and after high-T experiments

		Starting material			After high-T expts.		
Sample	x*	M_s (Am²/kg)	H_c (mT)	M_{rs}/M_s	M_s (Am²/kg)	H_c (mT)	M_{rs}/M_s
SP15	1	94.4	0.82	0.008	—	—	—
SP18	0.9	72.2	0.78	0.009	—	—	—
SP14	0.81	56.2	1.22	0.013	61.6	2	0.011
SP17	0.71	38.6	1.26	0.051	49.2	13.33	0.282
SP13	0.609	29.7	0.87	0.034	40.3	19.86	0.277
SP20	0.55	—	—	—	33.1	16.19	0.364
SP12	0.51	16.2	0.5	0.021	19.6	1.2	0.05
SP9	0.43	—	—	—	9.64	4.14	0.198

* Mole-fraction magnetite defined by ideal formula unit $(Fe_3O_4)_x(MgAl_2O_4)_{1-x}$.

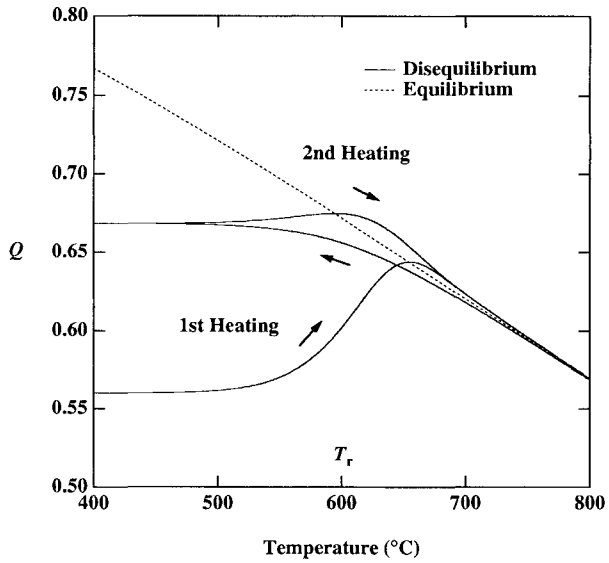

FIGURE 5. Schematic variation of nonconvergent cation order parameter, Q (solid lines), vs. temperature, T (°C), during temperature-sweep experiments (heating and cooling rate 10 °C/min). The solid curves are calculated values based on kinetic theory (Carpenter and Salje 1989). Dashed line is the equilibrium variation of Q with T (Carpenter and Salje 1994). Arrows indicate the directions of heating and cooling for first and subsequent experiments. T_r is the cation-distribution relaxation temperature, corresponding to a rapid increase in Q toward the equilibrium value.

at $T \approx 900$ °C. The initial value of Q in the susceptibility experiments is therefore lower than the equilibrium value at 650 °C, and there is a thermodynamic driving force for ordering. The kinetic behavior of Fe-rich spinels containing Mg and Al has been studied by Sujata and Mason (1992). Measurements of electrical resistivity on initially disordered material heated at a rate of 20 °C/min display enhanced resistivity at a characteristic relaxation temperature. The relaxation temperature is associated with the onset of rapid cation ordering. After heating above the relaxation temperature, Q may eventually reach its equilibrium value, which is maintained on cooling to room temperature.

For sample SP12 ($x = 0.51$) relaxation of the cation distribution occurs after heating to 650 °C. The difference in Q before and after relaxation yields an increase in T_C of approximately 70 °C, suggesting that there is strong interaction between magnetic and cation ordering in this system. This behavior contrasts with that of the titanomagnetite solid solution in which there is little variation in T_C for different degrees of cation order (Moskowitz 1987). The essential difference between the two systems is that the titanomagnetite solid solution contains nonmagnetic Ti atoms exclusively on B sites. The J_{AB} interaction is insensitive to variations in the distribution of Fe^{2+} and Fe^{3+} ions between A and B sites. In the magnetite-spinel solid solution Mg and Al atoms disorder between A and B sites, strongly affecting the J_{AB} interaction and hence T_C.

For many samples with nonreversible χ-T curves a second measurement was performed (dashed lines in Fig. 1). Sample SP13 (Fig. 1b) exsolved during the first experiment to yield an array of single-domain magnetic particles with T_C in the range 519–528 °C. The magnetic transition in this material displayed thermal hysteresis behavior during the second measurement experiment. T_C measured during heating is 528.3 °C. The value of T_C measured during cooling is 518.9 °C for experiment 1 and 518 °C for experiment 2. There appears to be a reversible difference between T_C measured when T is sweeping up and that measured when T is sweeping down. This thermal hysteresis behavior is observed in samples SP14, SP17, SP13, SP12, and SP9. The effect is most pronounced in sample SP14 ($x = 0.81$), where the difference between T_C for heating and cooling is 24.5 °C. Thermal hysteresis is often observed in temperature-sweep experiments when the sample temperature is unable to change at the same rate as the furnace temperature (thermal lag). This is not the case in these experiments because no thermal lag is observed in samples SP15 and SP18. Because hysteresis is reversible the effect is probably the result of a reversible difference in the state of cation order during heating and cooling. The behavior of sample SP12 discussed above suggests that T_C is higher for larger values of Q (i.e., a more ordered cation distribution), and hence samples displaying hysteresis have $Q_{heating} > Q_{cooling}$.

A schematic representation of the changes in Q during heating and cooling at 10 °C/min is shown in Figure 5. This figure is the result of a computer simulation of cation ordering during constant heating- and cooling-rate experiments, using the kinetic theory of Carpenter and Salje (1989) and the thermodynamic description of ordering in $MgAl_2O_4$ given by Carpenter and Salje (1994). Kinetic changes in Q are defined by the Ginzburg-Landau equation

$$\frac{dQ}{dt} = -\frac{\gamma \exp(-\Delta G^*/RT)}{2RT}\frac{\partial G}{\partial Q} \quad (1)$$

where γ is a constant and ΔG^* is the free energy of activation. G is the excess free energy due to ordering (relative to the disordered phase) given by

$$G = -hQ + \tfrac{1}{2}a(T - T_C)Q^2 + \tfrac{1}{6}cQ^6 \quad (2)$$

where h, a, c, and T_C are constants. Substituting Equation 2 into Equation 1 and integrating we obtain

$$t - t_0 = \int_{Q_0}^{Q} \frac{-2RT}{\gamma \exp(-\Delta G^*/RT)}\left[\frac{1}{-h + a(T - T_C)Q + cQ^5}\right]dQ \quad (3)$$

which may be solved numerically to obtain the behavior during either isothermal annealing or temperature-sweep experiments. Further details of these calculations are given elsewhere. Values for the constants h, a, c, and T_C were

taken from Carpenter and Salje (1994). Measured values for the kinetic constants γ and ΔG^* were not available. An approximate value for $\gamma = 3.84 \times 10^9$ s^{-1} was derived by fitting the Landau model to the kinetic data of O'Neill (1994) for $MgFe_2O_4$. A value of $\Delta G^* = 200$ kJ/mol was then chosen to yield a relaxation temperature in the range 500–600 °C.

The dashed line in Figure 5 represents the equilibrium variation of Q with T. The initial value of Q is lower than equilibrium in material quenched from high temperatures. There is a large thermodynamic driving force for ordering, but below 400 °C Q is prevented from increasing by kinetic constraints. As the temperature is swept above the range 500–600 °C Q rapidly increases toward its equilibrium value. This increase corresponds to the relaxation temperature identified by Sujata and Mason (1992). In a temperature-sweep experiment Q oversteps its equilibrium value because the rate of ordering tends to zero as equilibrium is approached. Q relaxes toward its equilibrium value only as the rate of ordering increases at higher temperatures.

The variation of Q with T during cooling from the high-temperature equilibrium value is indicated by the arrows in Figure 5. As T decreases, the rate of ordering becomes insufficient to allow Q to follow the equilibrium pathway. Below 500 °C Q remains constant and the degree of order is quenched. The large difference between the initial value of Q and the value obtained after heating and cooling through the relaxation temperature is responsible for the increase in T_C observed in sample SP12 (Fig. 1c). If a second experiment is performed on the sample with the new starting value of Q then the hysteresis behavior is revealed. Q begins to increase again when T approaches the relaxation temperature. The equilibrium value of Q is overstepped, and Q eventually relaxes toward equilibrium at high temperatures. All subsequent heating and cooling cycles follow the same Q-T path. If T_C coincides with the temperature range where $Q_{heating} > Q_{cooling}$ then the magnetic transition also displays thermal hysteresis.

Implications

The large variation in T_C with degree of cation order has implications for the calibration of T_C vs. composition (Fig. 2). No conclusions about the composition of an unknown phase can be made from a measurement of T_C unless Q is known and a calibration of T_C vs. Q has been performed. This may be relevant for other spinels in which nonmagnetic ions disorder between A and B sites. In terms of natural magnetic spinels (titanomagnetite), it is generally assumed from crystal-chemical arguments that Ti^{4+} ions exist only on octahedral B sites (Waychunas 1991). However, significant amounts of tetrahedrally coordinated Ti were suggested by Allan et al. (1989) in fully oxidized titanomagnetite (titanomaghemite). Hence, there may be more interaction between cation ordering and magnetism in this material, an effect that should not be ignored when interpreting the magnetic properties of naturally oxidized material. Significant amounts of Mg and Al can occur in titanomagnetite (Nishitani 1981). The presence of these cations on tetrahedral sites may also greatly affect magnetic properties.

This study has demonstrated that exsolution can be easily produced in the magnetite-spinel solid solution and that there is significant interaction between the resultant microstructures and the magnetic hysteresis properties. This has implications for rock magnetism because the microstructures are analogous to those often seen in natural titanomagnetites. A detailed study of subsolvus exsolution in the titanomagnetite solid solution has not been possible because of kinetic constraints. Current knowledge of the magnetic consequences of exsolution is based on a few studies of natural material. This work has studied a synthetic analog system with well-characterized starting material and known thermal histories.

Acknowledgments

All magnetic measurements were made at the Institute for Rock Magnetism (IRM), Minneapolis, with the aid of a grant from the University of Minnesota. R.J.H. wishes to thank the IRM for the use of its facilities and Chris Hunt for his help in performing the experiments. The IRM is funded by the Keck Foundation, the National Science Foundation, and the University of Minnesota. The authors thank G.L. Nord and M.E. Evans for their reviews of the manuscript. R.J.H. acknowledges the receipt of a grant from the Natural Environment Research Council.

References cited

Allan, J.E.M., Coey, J.M.D., Sanders, I.S., Schwertmann, U., Freidrich, G., and Wiechowski, A. (1989) An occurrence of a fully-oxidized natural titanomaghemite in basalt. Mineralogical Magazine, 53, 299–304.

Brown, N.E., Navrotsky, A., Nord, G.L., Jr., and Banerjee, S.K. (1993) Hematite-ilmenite (Fe_2O_3-$FeTiO_3$) solid solutions: Determinations of Fe-Ti order from magnetic properties. American Mineralogist, 78, 941–951.

Carpenter, M.A., and Salje, E. (1989) Time-dependent Landau theory for order/disorder processes in minerals. Mineralogical Magazine, 53, 483–504.

Carpenter, M.A., Powell, R., and Salje, E.K.H. (1994) Thermodynamics of nonconvergent cation ordering in minerals: I. An alternative approach. American Mineralogist, 79, 1053–1067.

Carpenter, M.A., and Salje, E.K.H. (1994) Thermodynamics of nonconvergent cation ordering in minerals: II. Spinels and the orthopyroxene solid solution. American Mineralogist, 79, 1068–1083.

Davis, P.M., and Evans, M.E. (1976) Interacting single-domain properties of magnetite intergrowths. Journal of Geophysical Research, 81, 989–994.

Dieckmann, R. (1982) Defects and cation diffusion in magnetite: IV. Nonstoichiometry and point defect structure of magnetite ($Fe_{3-\delta}O_4$). Berichte Bunsengesellschaft Physikalische Chemie, 81, 414–419.

Dunlop, D.J. (1973) Superparamagnetic and single-domain threshold sizes in magnetite. Journal of Geophysical Research, 78, 1780–1793.

——— (1974) Thermal enhancement of magnetic susceptibility. Journal of Geophysics, 40, 439–451.

Evans, M.E., and Wayman, M.L. (1974) An investigation of the role of ultra-fine titanomagnetite intergrowths in paleomagnetism. Geophysical Journal of the Royal Astronomical Society, 36, 1–10.

Harrison, R.J., and Putnis, A. (1995) Magnetic properties of the magnetite-spinel solid solution: Saturation magnetization and cation distributions. American Mineralogist, 80, 213–221.

Lehmann, J., and Roux, J. (1986) Experimental and theoretical study of $(Fe^{2+}Mg)(AlFe^{3+})_2O_4$ spinels: Activity-composition relationships, miscibility gaps, vacancy contents. Geochimica et Cosmochimica Acta, 50, 1765–1783.

Livingston, J.D. (1981) Microstructure and coercivity of permanent-magnet materials. Progress in Materials Science, 41a, 243–267.

Mattioli, G.S., Wood, B.J., and Carmichael, I.S.E. (1987) Ternary-spinel volumes in the system $MgAl_2O_4$-Fe_3O_4-$\gamma Fe_{8/3}O_4$: Implications for the effect of P on intrinsic f_{O_2} measurements of mantle-xenolith spinels. American Mineralogist, 72, 468–480.

Mattioli, G.S., and Wood, B.J. (1988) Magnetite activities across the $MgAl_2O_4$-Fe_3O_4 spinel join with application to thermobarometric estimates of upper mantle oxygen fugacity. Contributions to Mineralogy and Petrology, 98, 148–162.

Milliard, R.L., Peterson, R.C., and Hunter, B.K. (1992) Temperature dependence of cation disorder in $MgAl_2O_4$ spinel using ^{27}Al and ^{17}O magic-angle spinning NMR. American Mineralogist, 77, 44–52.

Moskowitz, B.M. (1987) Towards resolving the inconsistencies in characteristic physical properties of synthetic titanomaghemites. Physics of the Earth and Planetary Interiors, 46, 173–183.

Nafziger, R.H., Ulmer, G.C., and Woermann, E. (1971) Gaseous buffering for the control of oxygen fugacity at one atmosphere pressure. In G.C. Ulmer, Ed., Research techniques for high pressure and high temperature, p. 9–41. Springer-Verlag, New York.

Nell, J., and Wood, B.J. (1989) Thermodynamic properties in a multicomponent solid solution involving cation disorder: Fe_3O_4-$MgFe_2O_4$-$MgAl_2O_4$ spinels. American Mineralogist, 74, 1000–1015.

Nell, J., Wood, B.J., and Mason, T.O. (1989) High-temperature cation distributions in Fe_3O_4-$MgAl_2O_4$-$MgFe_2O_4$-$FeAl_2O_4$ spinels from thermopower and conductivity measurements. American Mineralogist, 74, 339–351.

Nishitani, T. (1981) Magnetic properties of titanomagnetites containing spinel ($MgAl_2O_4$). Journal of Geomagnetism and Geoelectricity, 33, 171–179.

O'Neill, H. (1994) Kinetics of cation order-disorder in $MgFe_2O_4$ spinel. European Science Foundation Program on Kinetic Processes in Minerals and Ceramics, Proceedings of a workshop on kinetics of cation ordering, Cambridge, U.K.

O'Neill, H.S.C., and Navrotsky, A. (1984) Cation distributions and thermodynamic properties of binary spinel solid solutions. American Mineralogist, 69, 733–753.

O'Reilly, W. (1984) Rock and mineral magnetism, 220 p. Blackie, Glasgow, U.K.

Peterson, R.C., Lager, G.A., and Hitterman, R.L. (1991) A time-of-flight neutron powder diffraction study of $MgAl_2O_4$ at temperatures up to 1273 K. American Mineralogist, 76, 1455–1458.

Price, G.D. (1980) Exsolution microstructures in titanomagnetites and their magnetic significance. Physics of the Earth and Planetary Interiors, 23, 2–12.

Readman, P.W., and O'Reilly, W. (1972) Magnetic properties of oxidised (cation deficient) titanomagnetites $(Fe,Ti,\square)_3O_4$. Journal of Geomagnetism and Geoelectricity, 24, 69–90.

Sack, R.O., and Ghiorso, M.S. (1991) An internally consistent model for the thermodynamic properties of Fe-Mg-titanomagnetite-aluminate spinels. Contributions to Mineralogy and Petrology, 106, 474–505.

Shive, P.N., and Butler, R.F. (1969) Stresses and magnetostrictive effects of lamellae in the titanomagnetite and ilmenohematite series. Journal of Geomagnetism and Geoelectricity, 21, 781–796.

Stephenson, A. (1969) The temperature dependent cation distribution in titanomagnetites. Geophysical Journal of the Royal Astronomical Society, 18, 199–210.

——— (1972) Spontaneous magnetization curves and Curie points of spinel containing two types of magnetic ion. Philosophical Magazine, 25, 1213–1232.

Stoner, E.C., and Wohlfarth, E.P. (1948) A mechanism of magnetic hysteresis in heterogeneous alloys. Philosophical Transactions of the Royal Society (London), 240A, 599.

Sujata, K., and Mason, T.O. (1992) Kinetics of cation redistribution in ferrospinels. Journal of the American Ceramic Society, 75, 557–562.

Trestman-Matts, A., Doris, S.E., and Mason, T.O. (1983) Thermoelectric determination of cation distribution in Fe_3O_4-$MgFe_2O_4$. Journal of the American Ceramic Society, 67, 69–74.

Tucker, P., and O'Reilly, W. (1980) The laboratory simulation of deuteric oxidation of titanomagnetites: Effect on magnetic properties and stability of thermoremanence. Physics of the Earth and Planetary Interiors, 23, 112–133.

Waychunas, G.A. (1991) Crystal chemistry of oxides and oxyhydroxides. Mineralogical Society of America Reviews in Mineralogy, 25, 11–68.

Wood, B.J., Kirkpatrick, R.J., and Montez, B. (1986) Order-disorder phenomena in $MgAl_2O_4$ spinel. American Mineralogist, 71, 999–1006.

Zijlstra, H. (1982) Permanent magnets: Theory. In E.P. Wohlfarth, Ed., Ferro-magnetic materials: A handbook of the properties of magnetically ordered substances, p. 38–105. North-Holland, Amsterdam.

Manuscript received May 11, 1995
Manuscript accepted November 6, 1995